



Revisiting brain iron deficiency in restless legs syndrome using magnetic resonance imaging

Vincent Beliveau^{a,b}, Ambra Stefani^a, Christoph Birkl^c, Christian Kremser^d, Elke R. Gizewski^{c,d}, Birgit Högl^a, Christoph Scherfler^{a,b,*}

^a Medical University of Innsbruck, Department of Neurology, Innsbruck, Austria

^b Medical University of Innsbruck, Neuroimaging Research Core Facility, Innsbruck, Austria

^c Medical University of Innsbruck, Department of Neuroradiology, Innsbruck, Austria

^d Medical University of Innsbruck, Department of Radiology, Innsbruck, Austria

ARTICLE INFO

Keywords:

RLS
MRI
Iron
Meta-analysis
Quantitative brain MRI

ABSTRACT

Study objectives: Studies on brain iron content in restless legs syndrome (RLS) using magnetic resonance imaging (MRI) are heterogeneous. In this study, we sought to leverage the availability of a large dataset including a range of iron-sensitive MRI techniques to reassess the association between brain iron content and RLS with added statistical power and to compare these results to previous studies.

Methods: The relaxation rates R_2 , R_2' , and R_2^* and quantitative susceptibility are MRI parameters strongly correlated to iron content. In general, these parameters are sensitive to magnetic field variations caused by iron particles. These parameters were quantified within iron-rich brain regions using a fully automatized approach in a cohort of 72 RLS patients and individually age and gender-matched healthy controls identified from an existing dataset acquired at the Sleep Laboratory of the Department of Neurology, Medical University of Innsbruck. 3 T-MRI measures were corrected for age and volume of the segmented brain nuclei and results were compared with previous findings in a meta-analysis.

Results: In our cohort, RLS patients had increased R_2^* signal in the caudate and increased quantitative susceptibility signal in the putamen and the red nucleus compared to controls, suggesting increased iron content in these areas. The meta-analysis revealed no significant pooled effect across all brain regions. Furthermore, potential publication bias was identified for the substantia nigra.

Conclusions: Normal and increased iron content of subcortical brain areas detected in this study is not in line with the hypothesis of reduced brain iron storage, but favors CSF investigations and *post mortem* studies indicating alteration of brain iron mobilization and homeostasis in RLS.

1. Introduction

Restless legs syndrome (RLS) is a sensorimotor disorder characterized by unpleasant sensations usually localized in the lower limbs, which begin at rest, worsen in the evening, and are relieved by movement (Allen et al., 2014). The prevalence of RLS was estimated to be between 5.5% and 11.6% in the general adult population of western countries (Koo, 2015; Didriksen et al., 2017). The pathophysiological mechanisms underlying RLS are not fully understood. Cumulative data from clinical observations, imaging, cerebrospinal fluid (CSF), and autopsy studies point toward the involvement of dysregulated circadian dynamics of dopamine release (Earley et al., 2014; Earley et al., 2017) and brain iron

metabolism (Allen et al., 2001; Earley et al., 2000; Earley et al., 2006; Connor et al., 2011; Rizzo et al., 2017), acting on a genetic predisposing background (Schormair et al., 2017).

RLS prevalence is high in conditions associated with iron deficiency or altered iron homeostasis such as iron deficiency anemia, end stage renal disease, or pregnancy, leading to the hypothesis that iron plays a key role in RLS pathophysiology. In addition, iron substitution resulted in relief and remission of RLS symptoms (Bae et al., 2021; Yang et al., 2019; Avni et al., 2019). Moreover, brain iron deficiency influences the glutamatergic and adenosine systems. On one side, it leads to increased glutamatergic tone, with subsequent functional impairment of corticostriatal-thalamic-cortical circuits in genetically vulnerable individuals

* Corresponding author at: Department of Neurology, Medical University Innsbruck, Anichstrasse 35, 6020 Innsbruck, Austria.

E-mail address: christoph.scherfler@i-med.ac.at (C. Scherfler).

<https://doi.org/10.1016/j.nicl.2022.103024>

Received 23 January 2022; Received in revised form 7 April 2022; Accepted 24 April 2022

Available online 26 April 2022

2213-1582/© 2022 The Author(s). Published by Elsevier Inc. This is an open access article under the CC BY-NC-ND license (<http://creativecommons.org/licenses/by-nc-nd/4.0/>).

(Lanza et al., 2022). On the other side, brain iron deficiency decreases adenosine tone (Lanza and Ferri, 2019), with subsequent dopaminergic impairment (responsible for sensorimotor dysfunction) and hyperglutamatergic tone (with subsequent hyperarousal state) (Ferré et al., 2017). In order to evaluate iron metabolism in RLS patients, serum and CSF measures (Earley et al., 2000), autopsy assessment of brain iron content (Earley et al., 2014; Connor et al., 2003), transcranial parenchymal ultrasound (Schmidauer et al., 2005; Godau et al., 2007), and magnetic resonance imaging (MRI) measurements (Allen et al., 2001; Earley et al., 2006) were undertaken by previous studies. This growing body of evidence suggest a strong association between brain iron deficiency and the occurrence of RLS symptoms (Gonzalez-Latapi and Malkani, 2019).

MRI allows for the quantification of non-heme iron storage in the brain using sequences sensitive to tissue magnetic susceptibility. Its main advantage compared to transcranial ultrasound, the only other imaging method for in vivo assessment of brain iron, is to provide increased spatial resolution and signal-to-noise. In patients with RLS, several brain MRI studies have reported lower iron content in the substantia nigra compared to healthy controls (Allen et al., 2001; Earley et al., 2006; Rizzo et al., 2013; Moon et al., 2014; Moon et al., 2015). Other studies have reported the absence of significant changes in iron-related MRI signal in the substantia nigra (Moon et al., 2014; Moon et al., 2015; Knake et al., 2010; Astrakas et al., 2008; Margariti et al., 2012). For other brain regions, results are mixed with evidence of significant increases, decreases, or no change and there is no clear association reported across studies (Allen et al., 2001; Earley et al., 2006; Rizzo et al., 2013; Moon et al., 2014; Moon et al., 2015; Knake et al., 2010; Astrakas et al., 2008; Margariti et al., 2012; Godau et al., 2008; Li et al., 2016).

Clinical inhomogeneity, small sample size, and technical considerations as well as differences between early and late disease onset have been suggested as possible sources responsible for the discrepancies across MRI studies (Rizzo and Plazzi, 2018). Unfortunately, although these explanations are plausible, they remain practically impossible to replicate based on published results. Thus, further studies with i) stringent inclusion and exclusion criteria, ii) adequate phenotypic characterization of RLS patients regarding age of onset, treatment, family history of RLS, associated conditions, as well as blood iron status, iii) sufficient group sizes, and iv) standardized MRI methods, are necessary to clarify brain iron content in patients with RLS.

In this study, we leverage the availability of a large dataset ($n = 72$) containing iron-sensitive MRI parameters (R_2 , R_2^* , R_2' , and quantitative susceptibility mapping; QSM) from RLS patients and individually age- and gender-matched healthy controls (Stefani et al., 2019) to reassess the brain iron content in RLS. To our knowledge, this is the largest repository of this kind across reported RLS studies. The statistical power provided by the sample size of this dataset combined with the range of available MR modalities allows us to present a sensitive and unified perspective to characterize the iron storage measured with MRI in subcortical brain regions in RLS. Finally, to interpret our results in the context of previous studies, we provide a *meta-analysis* reviewing the current evidence on brain iron content assessed with MRI in patients with RLS.

2. Methods

2.1. Subjects

A cohort of 72 patients with RLS was retrospectively identified from an existing dataset acquired at the Sleep Laboratory of the Department of Neurology, Medical University of Innsbruck (Stefani et al., 2019). Inclusion criteria were age > 18 years, and a diagnosis of RLS according to the current International Restless Legs Syndrome Study Group (IRLSSG) criteria (Allen et al., 2014). Mimics were excluded during a clinical interview performed by an expert in sleep medicine (AS).

Exclusion criteria were claustrophobia preventing MRI, RLS associated with end stage renal deficiency or heart failure, other neurological diseases identified through clinical examination and conventional MRI, white matter lesions of Fazekas score > 1 (Fazekas et al., 1991), iron supplementation during the previous 6 months, or current opioid or alpha-2-delta ligand medication. A cohort of 72 individually age- and sex-matched healthy controls were selected from the same database. Inclusion criteria for healthy control subjects were age > 18 years, absence of any relevant medical condition. Exclusion criteria were iron supplementation during the previous 6 months, any symptoms of RLS (evaluated during a clinical interview performed by an expert in sleep medicine), and positive family history for RLS in order to limit possible inclusion of carriers of genetic risk factors for RLS.

The study was performed according to the Declaration of Helsinki and approved by the ethics committee of the Medical University of Innsbruck. All subjects included in this study signed an informed consent form. However, as data sharing was not included in the original ethics, the data used in this study cannot be made available publicly due to privacy issues.

2.2. MRI data acquisition

MRI measurements were performed on a 3.0 Tesla whole-body MR scanner (Magnetom Verio, Siemens, Erlangen, Germany) with a 12 channel head-coil. All participants underwent the same MRI protocol, including the following sequences: a coronal 3D T_1 -weighted magnetization prepared rapid gradient echo sequence (repetition time (TR) = 1,800 ms; echo time (TE) = 2.19 ms; inversion time (TI) = 900 ms; flip angle (FA) = 9° ; matrix = $416 \times 160 \times 512$; voxel size = $0.43 \text{ mm} \times 1.2 \text{ mm} \times 0.43 \text{ mm}$; bandwidth = 199 Hz/pixel), a transversal 2D T_2 -weighted dual-echo turbo spin-echo (TSE) sequence (TR = 3,050 ms; TE₁ = 11 ms, TE₂ = 101 ms; FA = 150° ; matrix = $318 \times 384 \times 50$; voxel size = $0.57 \text{ mm} \times 0.57 \text{ mm} \times 3.0 \text{ mm}$; bandwidth = 213 Hz/pixel), a transversal 3D single-echo GRE sequence (TR = 28 ms; TE = 20 ms; FA = 15° ; matrix = $260 \times 320 \times 64$; voxel size = $0.69 \text{ mm} \times 0.69 \text{ mm} \times 2.4 \text{ mm}$; bandwidth = 120 Hz/pixel; GRAPPA factor = 2), a transversal 2D multi-echo gradient echo (GRE) sequence (TR = 200 ms; TE = 2.58, 4.81, 7.04, 9.27, 11.5, 13.73, 15.96, and 18.19 ms; FA: 20° ; matrix: $208 \times 256 \times 43$; voxel size = $0.86 \text{ mm} \times 0.86 \text{ mm} \times 3.75 \text{ mm}$; bandwidth = 814 Hz/pixel) and a diffusion-weighted sequence with 20 directions, $b_{\text{val}} = 1000 \text{ mm}^2/\text{s}$ and one b_0 image (TR = 6,300 ms; TE = 95 ms; FA: 90° ; matrix: $256 \times 256 \times 45$; voxel size = $0.9 \text{ mm} \times 0.9 \text{ mm} \times 3.3 \text{ mm}$; bandwidth = 1502 Hz/pixel; GRAPPA factor = 2). Susceptibility-weighted (SW) images were obtained directly by the scanner from the single-echo GRE sequence.

2.3. Quantification of R_2 , R_2^* , R_2' and QSM

To account for subject motion, all echos from the GRE and TSE sequences were rigidly realigned (cubic interpolation) to the first echo using ANTs (v2.3.4, <http://stnava.github.io/ANTs/>) motion correction script. R_2 maps were calculated using the relation $R_2 = \log(S_{TE1}/S_{TE2}) / (TE_2 - TE_1)$, where $S_{TE1/2}$ denote the signal of the voxel at the first and second echos and $TE_{1/2}$ denote the echo times. R_2^* maps were calculated by voxel-wise fitting of a mono-exponential model to the signal values of the respective gradient echos. R_2' maps were obtained using the relation: $R_2^* = R_2 + R_2'$.

The phase images of the multi-echo GRE sequence were not available for calculating QSM maps, therefore, the homodyne-filtered phase images of the single-echo GRE sequence were used instead. However, as standard QSM algorithms applied to filtered GRE phase images do not provide quantitative measures of susceptibility, we have trained a convolutional neural network, termed HFP-QSMGAN (<https://github.com/mui-neuro/HFP-QSMGAN>), to solve the compounded problem of 1) computing the solution to the inverse dipole problem, and 2) compensating for the effects of the homodyne filtering. This model was inspired

by the QSMGAN framework recently proposed by Chen et al. (Chen et al., 2019) and was able to accurately solve the compounded problem of dipole inversion from filtered GRE phase images and correcting for the homodyne-filtering in order to predict regional QSM values. The regional susceptibility values predicted by this model were significantly correlated with ground truth in all regions aside from the thalamus; this region was thus excluded from further analysis. Regional QSM values were referenced to values from the posterior limb of the internal capsule (PLIC) (Straub et al., 2017). Detailed information on the architecture and training of the HFP-QSMGAN model and QSM quantification is available in the [Supplementary Material](#).

The caudate (CAU), pallidum (PAL), putamen (PUT), and thalamus (THA) were automatically labeled on the T_1 -weighted images using FreeSurfer (v6, <https://surfer.nmr.mgh.harvard.edu/>) (Fischl, 2012). The dentate nuclei (DEN), red nuclei (RN), substantia nigra (SN), and subthalamic nuclei (STN) were labeled on the SW images using FC-Dense Net models trained for individual region segmentation (Beliveau et al., 2021) (<https://github.com/mui-neuro/swi-cnn>). All labels were visually assessed and manually corrected where necessary. Individual maps of R_2 , R_2^* , R_2' , and QSM were aligned with the corresponding space using boundary-based registration (Greve and Fischl, 2009) and summary values were obtained by taking the regional means.

For each region, associations between mean regional MRI iron measures and age or volume were removed using a robust linear regression (`lmRob` from R's `robust` package v0.5–0.0). Firstly, significant associations with age or volume were identified by fitting independent models (including intercept) for each of the covariate in healthy controls. Then, significant covariates ($p < 0.05$) were included in a single summary model (including intercept) and the model was reestimated, again using data from healthy controls: the full regression model including both covariates was specified as `lmRob (regional_mean_iron ~ age + regional_volume)`. This summary model was then used to adjust the mean regional iron parameters from both RLS patients and healthy controls. Final summary values were obtained by averaging estimates from both the left and right hemispheres.

2.4. Statistics

All statistical analyses were performed in R (v4.1) (R Core Team, 2018). For all statistical tests, p -values < 0.05 were deemed significant. Normality was assessed using the Shapiro-Wilks test (Shapiro and Wilk, 1965). Wilcoxon rank-sum tests and Pearson's Chi-squared tests were used to compare demographics across groups where appropriate. Early onset was defined as before 45 years of age.

Differences in the MRI iron measures between healthy controls and RLS patients were uniformly assessed using Wilcoxon rank-sum tests. The significance of all comparisons was corrected for multiple comparisons using the false discovery rate (FDR) method (Benjamini and Hochberg, 1995). Further post hoc comparisons were performed using disease onset and drug status as subgroups of RLS. Group differences between healthy controls and RLS subgroups were assessed using Kruskal-Wallis test and the results were corrected for multiple comparisons using the FDR method.

Post hoc analyses investigating associations between regional iron-sensitive MRI parameters in RLS patients and demographic variables were assessed using Wilcoxon rank-sum tests and Spearman's correlations where appropriate. P -values were corrected using the FDR method.

2.5. Meta-analysis

Studies investigating iron deficiency in RLS using MRI were identified through a search on PubMed MEDLINE with the search term “(rls OR restless legs syndrome) AND iron AND MRI” completed on July 5th, 2021. Additionally, the references from several reviews were examined (Rizzo et al., 2017; Moon et al., 2014; Rizzo and Plazzi, 2018).

Random-effects models with Sidik-Jonkman estimator (Sidik and

Jonkman, 2007) and Q-profile method for the confidence intervals (Viechtbauer, 2007) were used to evaluate the pooled effects within and across studies. Sensitivity analyses, where the main pooled effect is recalculated, were performed using a leave-one-out procedure. Funnel plots were used to assess the distribution of standardized mean differences (SMD) relative to the standard error across studies and asymmetry was evaluated using Egger's test of the intercept (Egger et al., 1997). These analyses were performed using R's `meta` package (Schwarzer et al., 2007).

3. Results

3.1. Demographics and clinical information

Demographic details and clinical information are presented in [Table 1](#). All continuous parameters were found to violate the normality assumption as evaluated by the Shapiro-Wilks test; hence, nonparametric Wilcoxon rank sum tests were used. All comparisons were found to be non-significant.

3.2. Comparison of brain iron content between RLS & healthy controls

Mean regional iron measures (R_2 , R_2^* , R_2' , and QSM) were corrected for significant age or volume effects; the models used for correction are reported in [Supplementary Table S1](#). Corrected values are presented in [Fig. 1](#) and [Supplementary Table S2](#) for both RLS patients and healthy controls. Across all brain regions, there was no significant difference in regional R_2 and R_2' values between RLS and healthy controls. Regional R_2^* values were significantly greater for RLS patients compared to healthy controls in the caudate ($p = 0.006$, corrected) and for QSM in the putamen ($p = 0.006$, corrected), and red nucleus ($p = 0.004$, corrected). For these significant iron-sensitive MRI measures, post hoc analyses in the RLS group revealed no significant group difference of sex, onset (early/late), medication (untreated/dopaminergic) and family history, and no significant association with age, age at onset, disease duration, CGI, IRLS, RLS-6, family history, serum iron, serum ferritin, and serum transferrin saturation. Additional post hoc comparisons revealed no significant differences in iron-sensitive MRI parameters

Table 1
Demographics and clinical information.

	Healthy controls	RLS patients	P -value ¹
Sample size (N)	72	72	
Age (years), median (IQR)	51.0 (46.4–57.9)	51.9 (46.6–59.7)	0.52
Sex (male/female)	35/37	35/37	1.00
Onset (early/late)	–	46/26	
Age at onset (years), median (IQR)	–	37.0 (28.0–48.5)	
Disease duration (years), median (IQR)	–	14.8 (5.0–21.0)	
Drug status (untreated/dopaminergic)	–	29/43	
CGI, median (IQR)	–	3.5 (3.0–4.0)	
IRLS, median (IQR)	–	13.7 (7.0–21.5)	
RLS-6, median (IQR)	–	15.0 (8.0–20.0)	
Family history (yes/no)	–	28/44	
Iron ($\mu\text{mol/L}$), median (IQR)	17.6 (13.6–20.7)	18.0 (15.4–20.5)	0.38
Ferritin ($\mu\text{g/L}$), median (IQR)	109.9 (46.8–160.2)	129.6 (52.5–154.5)	0.50
Transferrin (mg/dL), median (IQR)	263.9 (243.0–281.0)	266.9 (235.0–293.0)	0.88
Transferrin saturation (%), median (IQR)	27.1 (21.0–32.0)	27.6 (20.0–33.2)	0.62

CGI: clinical global impression (0–7); IQR: Interquartile range; IRLS: International Restless Legs Syndrome Study Group rating scale; RLS: restless legs syndrome; RLS-6: Restless Legs Syndrome-6 Scale (0–60); Early onset was defined as before 45 years of age.

¹ Wilcoxon rank sum test; Pearson's Chi-squared test.

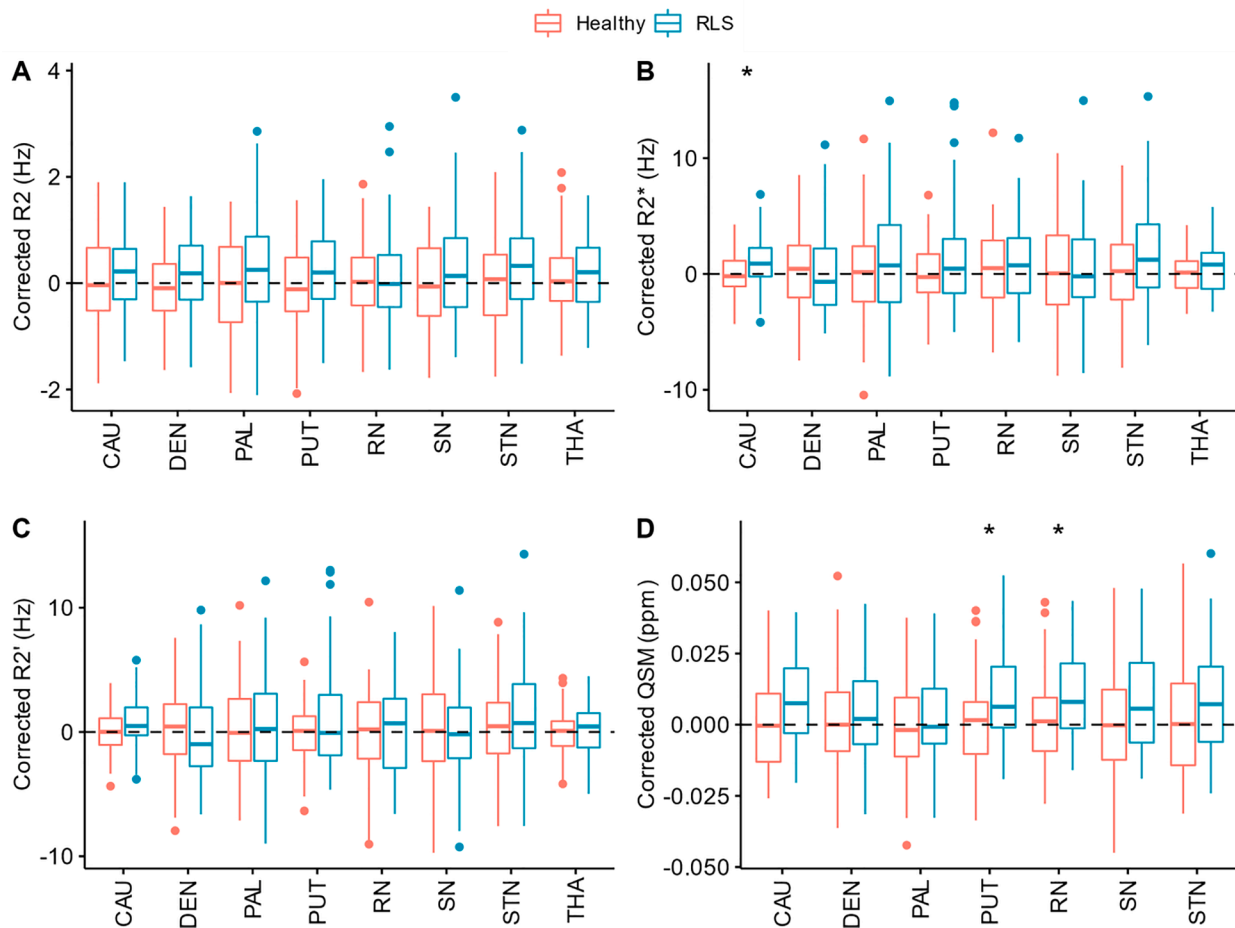


Fig. 1. Regional (A) R_2 , (B) R_2^* , (C) R_2' and (D) QSM values corrected for age and volume for healthy controls (blue) and RLS patients (red). CAU: Caudate, DEN: Dentate nuclei, PAL: Pallidum, PUT: Putamen, RN: Red nuclei, SN: Substantia Nigra, STN: Subthalamic Nuclei, THA: Thalamus. * $p < 0.05$, FDR corrected. (For interpretation of the references to colour in this figure legend, the reader is referred to the web version of this article.)

between healthy controls and RLS subgroups defined by disease onset and drug status.

3.3. Meta-analysis

The PRISMA flow chart (Fig. 2) provides an overview of the number of articles screened, included, and excluded. A total of 42 studies were identified from a database search. No additional study was identified through the additional examination of reviews. A total of 32 studies were excluded: 12 were reviews, 11 were not imaging studies or were not investigating brain iron, three did not report regional measures of iron, three were case reports, two were clinical trials including only patients, and one was a duplicate. Up to 2014, the remaining studies coincided exactly with a previous review presented by Moon et al. (Moon et al., 2014). Hence, a total of ten studies combined with our results were included in the meta-analysis. To increase the homogeneity with the other studies, results obtained with the semi-automated tracing method were used for the study of Moon et al. (Moon et al., 2015), and values referenced to CSF were used for the study of Knake et al. (Knake et al., 2010). Furthermore, although it is not explicitly stated, the two studies by Moon and colleagues (Moon et al., 2014; Moon et al., 2015) appear to investigate the same cohort, hence their reported effect sizes were pooled.

The random-effects model provided no significant pooled effect indicative of a difference in iron content between RLS and healthy controls in any of the brain regions (Fig. 3 and Supplementary Fig. S1). Only one other study (Margariti et al., 2012) had previously investigated

iron content within the subthalamic nuclei in RLS, hence, this region was excluded from the meta-analysis. Sensitivity analyses were performed by removing each study in turn and re-evaluating the random-effects model; significant results were observed only when omitting the current study, and significant pooled effects were observed for the putamen (Standardized Mean Difference (SMD) = -0.42, 95% CI = [-0.74, -0.11]), the red nucleus (SMD = -0.34, 95% CI = [-0.52, -0.15]), and the substantia nigra (SMD = -0.45, 95% CI = [-0.83, -0.07]). Forest plots presenting the data, the outcome of the random-effects models, and parameters from the studies are presented in Fig. 3 and supplementary Fig. S1. Heterogeneity (I^2) across studies ranged from 64% (moderate) to 87% (substantial) (Higgins et al., 2003); see Fig. 3 and Supplementary Fig. S1 for details.

Funnel plots presenting the SMD and corresponding standard error across studies are displayed in Fig. 4 for the substantia nigra and in Supplementary Fig. S2 for the other brain regions. Egger's tests indicated a substantial asymmetry for the substantia nigra ($t = -5.943$, $p = 0.0006$); this asymmetry was also present when excluding the current study ($t = -4.0$, $p = 0.0071$). No significant asymmetry was present for the other brain regions. However, the funnel plots highlighted the presence of outliers as well as an absence of small studies with small effect sizes for most brain regions.

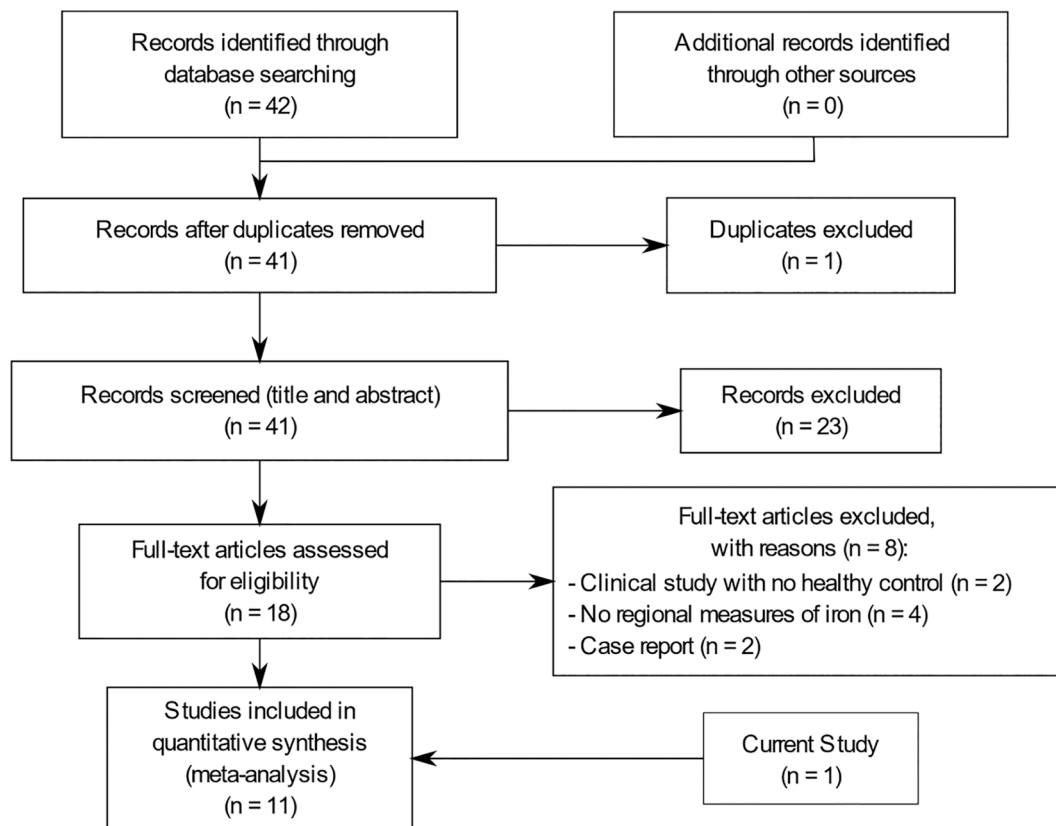


Fig. 2. Flow Diagram of the systematic search for MRI studies of iron in RLS.

4. Discussion

4.1. MRI findings

Our results indicated small, but significant regional increases of R_2^* in the caudate and of QSM in the putamen and red nucleus of RLS patients compared to healthy controls, which typically suggests increased iron content in these brain regions. These increases in R_2^* and QSM and the corresponding absence of any significant difference in the iron-sensitive parameters of other brain regions between RLS patients and healthy controls come as a sharp contrast with previous MRI studies. Furthermore, we did not observe any evidence of lower brain iron content in subgroups of the disease determined by disease onset (early and late) or drug status (unmedicated and dopaminergic treatment) which suggests that brain iron content remains unaltered across these clinical phenotypes of RLS and that it is not modified by dopaminergic treatment.

It is important to emphasize that, although the so-called iron-sensitive MRI parameters used in this study have been shown to be strongly correlated with post mortem iron measures (Langkammer et al., 2010; Langkammer et al., 2012), they represent the total contribution of paramagnetic, diamagnetic, and ferromagnetic signals from the tissue of interest and are therefore influenced by other properties than the presence of iron solely (Möller et al., 2019; Hametner et al., 2018). Furthermore, other aspects such as the iron oxidation state could further bias the quantification of iron with MRI. In a recent study (Birkl et al., 2020), it was shown that changes in iron oxidation state from ferric towards ferrous iron, in the absence of any change in total iron content, lead to an observable decrease in R_2 , R_2^* and QSM. Beyond these considerations, additional factors such as disease heterogeneity, disease stages, or even age-related effects could further contribute the differences observed across studies. In this context, it is not surprising to see that the significant differences observed between RLS patients and

healthy controls for R_2^* (caudate) and QSM (putamen and red nucleus) do not align and may reflect secondary factors unrelated to iron such as a differential involvement of aging-related process, e.g., changes in myelin content (Möller et al., 2019; Hametner et al., 2018; Treit et al., 2021). This hypothesis is in line with recent evidence of morphological alterations and atrophy within regions of the basal ganglia and the limbic system in RLS (Mogavero et al., 2021), supporting the concept of RLS as a complex network disorder, with the thalamus representing a crucial node within different networks, including the sensorimotor and limbic pathways. Ultimately, *post mortem* studies in large cohorts will be needed to fully elucidate the role of iron in RLS, independently of whether new methods to assess brain iron metabolism become available in the future.

A few limitations deserve to be acknowledged. Firstly, the QSM maps were quantified from filtered GRE phase images and may be less accurate than QSM quantified directly from unfiltered phase images. Therefore, these results need to be independently validated using a standard MRI sequence and modeling approach for QSM. Nonetheless, these data provide further characterization of susceptibility-related changes in RLS patients compared to healthy participants. Furthermore, approximation of R_2 using two echoes results in lower values compared to the gold standard using multiple single echo spin echo sequences. Nevertheless, the approximate R_2 values behave comparably to multi-echo spin echo estimates, so that for a group comparison this methodological bias can be neglected. Clinical heterogeneity across RLS patients is an additional concern. However, no significant differences in iron-sensitive MRI parameters between healthy controls and RLS subgroups defined by disease onset and drug status were found. It is therefore unlikely that clinical variability has influenced the association between brain iron content and RLS in the present study. Finally, polysomnography was not available for all subjects and, therefore, it was not included in this study as variable of interest to be correlated with MRI findings.

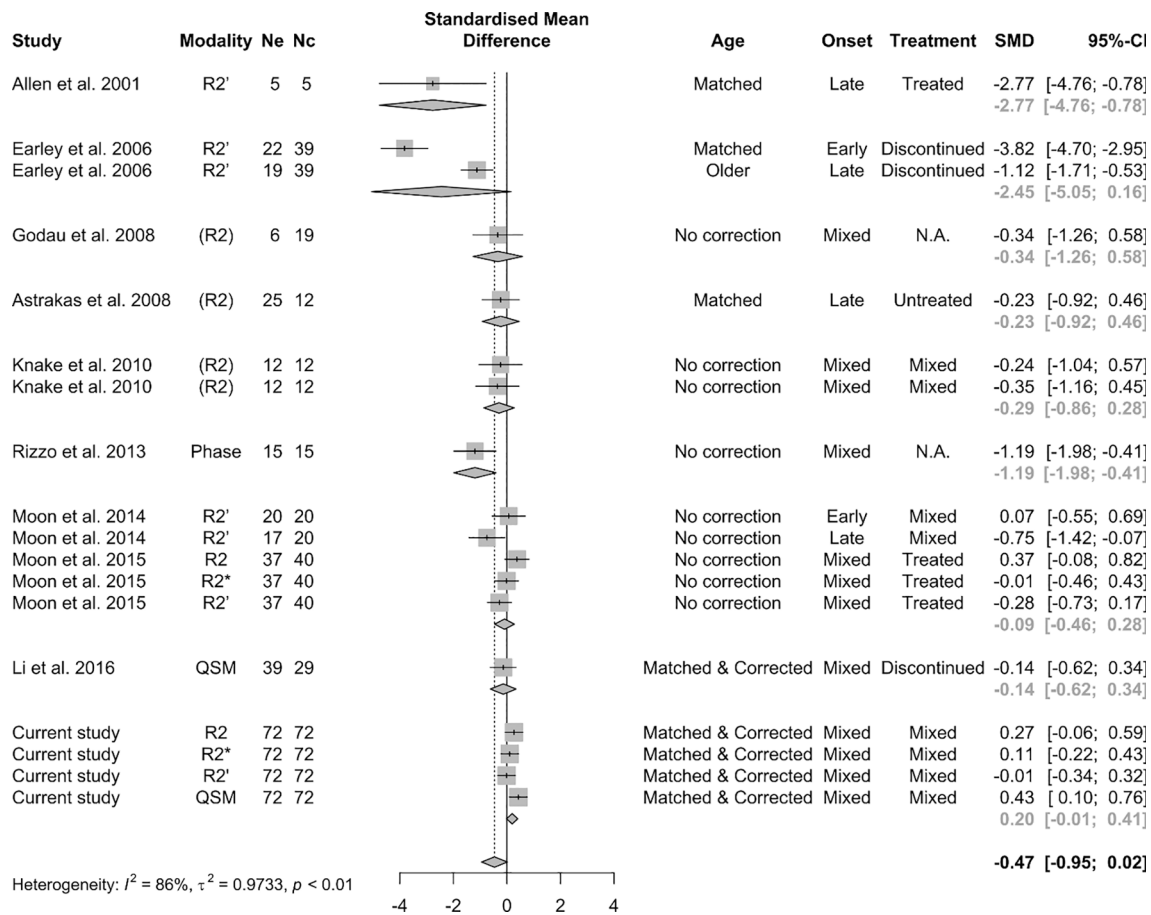


Fig. 3. Forest plot outlining the results of previous studies investigating iron deficiency in RLS with MRI for the substantia nigra and the caudate. The diamonds indicate the pooled effects estimated by the random-effects models. Mean and standard deviation for studies marked as (R₂) were estimated from reported T₂ values using the relation R₂ = 1/T₂. Note: Li. et al. have corrected their results for either age or volume, but did not indicate which was used specifically for each region. Ne: number of samples in RLS group, Nc: number of samples in the healthy control group, SMD: Standardized Mean Difference.

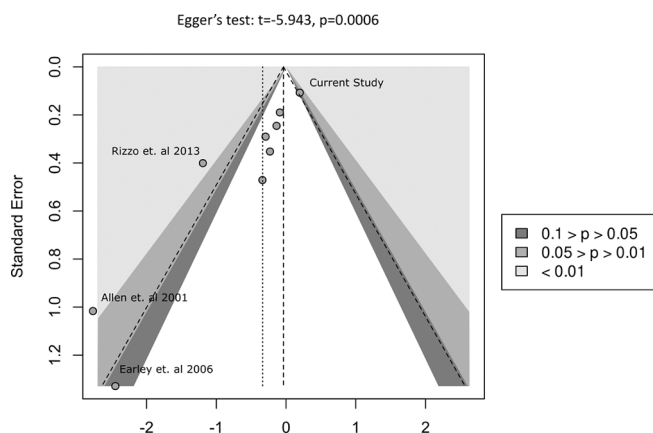


Fig. 4. Funnel plot presenting the pooled SMD of the different studies relative to their standard error for the substantia nigra. The different shadings (light, medium, and dark grey) represent respective confidence intervals. The vertical dashed lines indicate the estimated effect (left) and the null (center).

4.2. Meta-analysis

The results from our meta-analysis indicated that there is no cumulative evidence supporting the assumption of lower brain iron content in RLS patients compared to healthy controls across all investigated brain regions. This is surprising given that the results from MRI studies

reporting lower brain iron content in RLS are currently regarded as providing strong support for brain iron deficiency in RLS. The sensitivity analysis revealed that small, but significant negative pooled effects (i.e., lower iron in RLS) for the putamen, red nucleus and substantia nigra would have been observed, had the current study not been included in the model. However, substantial heterogeneity across studies was observed for all brain regions, and outliers can be seen to be driving these effects. This heterogeneity may have arisen from multiple factors. As discussed above, age and partial volume effects may have had a strong influence on the results. Furthermore, the use of different MRI sequences and image processing strategies, including the usage of manual methods, may also have been substantial sources of variability.

Significant funnel plot asymmetry was found for the substantia nigra, but not for other brain regions. Funnel plot asymmetry can arise from different sources including reporting biases, methodological differences, true heterogeneity, data irregularities, or even chance (Egger et al., 1997; Sterne et al., 2011). Two noticeable outliers for the substantia nigra come from the earliest studies on the topic (Allen et al., 2001; Earley et al., 2006). This is not surprising and is expected from early explorative studies. However, a noticeable absence of small studies with larger standard error is apparent from the funnel plots of most brain regions, which is usually interpreted as a publication bias (Song and Hooper, 2013). Indeed, small studies presenting a contradicting view to the well-established evidence of iron deficiency in RLS would have likely not been published due to their small statistical power. Unfortunately, even though studies indicating no evidence of lower brain iron content in RLS are often acknowledged by reviews on the topic, they are generally dismissed without quantitative argument. Nonetheless, in the

current *meta*-analysis 5 out of 8 previously reported studies (Fig. 3) did not find significant pooled evidence for lower iron content in the substantia nigra in RLS patients compared to healthy controls (Moon et al., 2014; Moon et al., 2015; Astrakas et al., 2008; Godau et al., 2008; Li et al., 2016). Taken together these results suggest that MRI-based evidence of iron deficiency in RLS should be regarded with care.

4.3. Implications for the field

The role of iron deficiency in RLS is supported by the high RLS prevalence in patients with iron-deficient anemia or with end-stage renal disease (Trenkwalder et al., 2016), as well as during pregnancy (Manconi et al., 2004) and by improvement of RLS symptoms with iron supplementation in these cases. Although this association has been reported already in 1953 by Nordlander (Nordlander, 1953), studies on iron content in patients with RLS started to be conducted only in the 1990s and have notably increased in number since then. Despite a large body of research, the pathogenetic mechanisms underlying the association between iron and RLS are still not fully understood.

Neuropathological studies suggested that in patients with RLS iron acquisition by the neuromelanin cells of the substantia nigra is impaired (Connor et al., 2003), leading to cellular iron deficiency (Connor et al., 2004). Moreover, in neuromelanin cells, substantia nigra, and putamen, the concentration of pro-hepcidin (a prohormone regulating iron efflux) was found to be increased (i.e., leading to iron deficiency) in RLS samples compared to healthy controls (Clardy et al., 2006). Studies investigating CSF iron parameter further support the concept that brain iron uptake is impaired in patients with RLS: reduced CSF ferritin and increased transferrin have been reported in RLS (Earley et al., 2000; Mizuno et al., 2005). These findings have been suggested to represent a compensatory response to the brain iron deficiency or a defective signaling mechanism (Clardy et al., 2006). In line with this hypothesis, Connor et al. (2011) reported a significant reduction of intracellular iron and ferritin, as well as a significant upregulation of transferrin receptor, in the epithelial cells of the choroid plexus, supporting that iron transport to the brain via transferrin is impaired in RLS.

Besides studies assessing iron sensitive parameters, the hypothesis of reduced brain iron storage in RLS is primarily grounded around the seminal work of Connor and colleagues (2003) (Connor et al., 2003). This study performed *post mortem* iron staining to quantify levels of iron in target brain regions; this technique is regarded as a gold standard. Nonetheless, these experiments were performed in a small cohort of RLS patients ($n = 7$) and were, to the best of our knowledge, never replicated. Additional evidence of reduced iron storage in RLS was provided by studies utilizing transcranial ultrasound to investigate hypoechogenicity of the substantia nigra in RLS patients (Schmidauer et al., 2005; Godau et al., 2007); it was shown that RLS patients exhibit reduced midbrain areas of hyperechogenicity. Compared to MRI, transcranial ultrasound offers substantially less spatial resolution and there is no quantitative evidence linking hypoechogenicity/hyperechogenicity to iron levels. As our *meta*-analysis indicated that MRI provides limited, and possibly biased evidence of reduced brain storage, further studies using more precise techniques to assess brain iron are needed to definitely clarify this issue.

It could be hypothesized that brain iron availability is functionally impaired in RLS, i.e., iron is available, but cannot be efficiently mobilized resulting in a functional deficiency, leading to reduced brain iron in severe cases. Along that line, Connor et al. (Connor et al., 2004)⁵⁸ also found a decrease in transferrin receptors in neuromelanin cells in RLS (which should be increased in iron insufficiency). The authors interpreted this as a functional deficit in the post-transcriptional regulatory mechanisms for transferrin receptor expression. Of note, increased serum levels of hepcidin and normal serum ferritin have been reported in RLS compared to controls (Chenini et al., 2020; Dauvilliers et al., 2018), possibly reflecting an iron homeostasis dysregulation rather than an absolute iron deficiency. Few studies have investigated

mitochondrial function in individuals with RLS. A pattern consistent with high iron turnover feeding an increased mitochondrial iron status and iron demand has been described, with mitochondrial iron surplus at the expense of cytosolic iron (Snyder et al., 2009). Reduced expression of mitochondrial iron genes and oxidative response genes, indicating reduced mitochondrial iron availability, has also been reported (Haschka et al., 2019). Both these studies suggest mitochondrial dysfunctionality in RLS.

Although our MRI findings do not provide evidence that brain iron mobilization or homeostasis is functionally altered in RLS, our results indicate that these mechanisms do not decrease brain iron storage as assessed by current state-of-the-art MRI measurements of brain iron content. The results of our study and the *meta*-analysis, as well as other findings of altered iron parameters in CSF and serum of RLS patients, suggest that iron pathology in RLS is far more complex than iron deficiency. Iron homeostasis dysregulation could be an alternative pathogenetic mechanism in RLS, but future studies are needed to further elucidate this topic.

CRediT authorship contribution statement

Vincent Beliveau: Conceptualization, Methodology, Software, Validation, Formal analysis, Data curation, Writing – original draft, Visualization. **Ambra Stefani:** Conceptualization, Writing – original draft. **Christoph Birkel:** Conceptualization, Writing – original draft. **Christian Kremser:** Writing – original draft. **Elke R. Gizewski:** Writing – original draft. **Birgit Högl:** Conceptualization, Resources, Writing – original draft. **Christoph Scherfler:** Conceptualization, Resources, Writing – original draft, Supervision, Project administration.

Declaration of Competing Interest

The authors declare the following financial interests/personal relationships which may be considered as potential competing interests: The study was funded by a Grant from Translational Research Fund of the government of Tyrol, Austria, to Birgit Högl and in-kind resources of the Medical University of Innsbruck. All authors report no conflict of interest.

Appendix A. Supplementary data

Supplementary data to this article can be found online at <https://doi.org/10.1016/j.nicl.2022.103024>.

References

- Allen, R.P.R.P., Barker, P.B.B., Wehrl, F., Song, H.K.K., Earley, C.J.J., 2001. MRI measurement of brain iron in patients with restless legs syndrome. *Neurology* 56 (2), 263–265. <https://doi.org/10.1212/WNL.56.2.263>.
- Allen, R.P., Picchiatti, D.L., Garcia-Borreguero, D., et al., 2014. Restless legs syndrome/Willis-Ekbom disease diagnostic criteria: updated International Restless Legs Syndrome Study Group (IRLSSG) consensus criteria – history, rationale, description, and significance. *Sleep Med.* 15 (8), 860–873. <https://doi.org/10.1016/j.sleep.2014.03.025>.
- Astrakas, L.G., Konitsiotis, S., Margariti, P., Tsouli, S., Tzarouhi, L., Argyropoulou, M.I., 2008. T2 relaxometry and fMRI of the brain in late-onset restless legs syndrome. *Neurology* 71 (12), 911–916. <https://doi.org/10.1212/01.wnl.0000325914.50764.a2>.
- Avni, T., Reich, S., Lev, N., Gafter-Gvili, A., 2019. Iron supplementation for restless legs syndrome – A systematic review and meta-analysis. *Eur. J. Int. Med.* 63 (February), 34–41. <https://doi.org/10.1016/j.ejim.2019.02.009>.
- Bae, H., Cho, Y.W., Kim, K.T., Allen, R.P., Earley, C.J., 2021. Randomized, placebo-controlled trial of ferric carboxymaltose in restless legs syndrome patients with iron deficiency anemia. *Sleep Med.* 84, 179–186. <https://doi.org/10.1016/j.sleep.2021.05.036>.
- Beliveau, V., Nørgaard, M., Birkel, C., Seppi, K., Scherfler, C., 2021. Automated segmentation of deep brain nuclei using convolutional neural networks and susceptibility weighted imaging. *Hum. Brain Mapp.* 42 (15), 4809–4822. <https://doi.org/10.1002/hbm.25604>.
- Benjamini, Y., Hochberg, Y., 1995. Controlling the false discovery rate: a practical and powerful approach to multiple testing. *J. R. Stat. Soc. Ser. B* 57 (1), 289–300. <https://doi.org/10.1111/j.2517-6161.1995.tb02031.x>.

- Birkel, C., Birkel-Toegelhofer, A.M., Kames, C., et al., 2020. The influence of iron oxidation state on quantitative MRI parameters in post mortem human brain. *Neuroimage* 220, 117080. <https://doi.org/10.1016/j.neuroimage.2020.117080>.
- Chen, Y., Jakary, A., Avadiappan, S., Hess, C.P., Lupo, J.M., 2019. QSMGAN: improved quantitative susceptibility mapping using 3D generative adversarial networks with increased receptive field. *Neuroimage* 2019 (207), 116389. <https://doi.org/10.1016/j.neuroimage.2019.116389>.
- Chenini, S., Delaby, C., Rassin, A.-L., et al., 2020. Hepcidin and ferritin levels in restless legs syndrome: a case-control study. *Sci. Rep.* 10 (1), 11914. <https://doi.org/10.1038/s41598-020-68851-0>.
- Clardy, S.L., Wang, X., Boyer, P.J., Earley, C.J., Allen, R.P., Connor, J.R., 2006. Is ferroportin-hepcidin signaling altered in restless legs syndrome? *J. Neurol. Sci.* 247 (2), 173–179. <https://doi.org/10.1016/j.jns.2006.04.008>.
- Connor, J.R., Boyer, P.J., Menzies, S.L., et al., 2003. Neuropathological examination suggests impaired brain iron acquisition in restless legs syndrome. *Neurology* 61 (3), 304–309. <https://doi.org/10.1212/01.WNL.0000078887.16593.12>.
- Connor, J.R., Wang, X.S., Patton, S.M., et al., 2004. Decreased transferrin receptor expression by neuromelanin cells in restless legs syndrome. *Neurology* 62 (9), 1563–1567. <https://doi.org/10.1212/01.WNL.0000123251.60485.AC>.
- Connor, J.R., Ponnuru, P., Wang, X.-S., Patton, S.M., Allen, R.P., Earley, C.J., 2011. Profile of altered brain iron acquisition in restless legs syndrome. *Brain* 134 (4), 959–968. <https://doi.org/10.1093/brain/awr012>.
- Dauvilliers, Y., Chenini, S., Vialaret, J., et al., 2018. Association between serum hepcidin level and restless legs syndrome. *Mov. Disord.* 33 (4), 618–627. <https://doi.org/10.1002/mds.27287>.
- Didriksen, M., Rigas, A.S., Allen, R.P., et al., 2017. Prevalence of restless legs syndrome and associated factors in an otherwise healthy population: results from the Danish Blood Donor Study. *Sleep Med.* 2017 (36), 55–61. <https://doi.org/10.1016/j.sleep.2017.04.014>.
- Earley, C.J.B., Barker, P., Horska, A., Allen, R.P., 2006. MRI-determined regional brain iron concentrations in early- and late-onset restless legs syndrome. *Sleep Med.* 7 (5), 458–461. <https://doi.org/10.1016/j.sleep.2005.11.009>.
- Earley, C.J., Connor, J.R., Beard, J.L., Malecki, E.A., Epstein, D.K., Allen, R.P., 2000. Abnormalities in CSF concentrations of ferritin and transferrin in restless legs syndrome. *Neurology* 54 (8), 1698–1700. <https://doi.org/10.1212/WNL.54.8.1698>.
- Earley, C.J., Connor, J., Garcia-Borreguero, D., et al., 2014. Altered brain iron homeostasis and dopaminergic function in restless legs syndrome (Willis-Ekbom Disease). *Sleep Med.* 15 (11), 1288–1301. <https://doi.org/10.1016/j.sleep.2014.05.009>.
- Earley, C.J., Uhl, G.R., Clemens, S., Ferré, S., 2017. Connectome and molecular pharmacological differences in the dopaminergic system in restless legs syndrome (RLS): plastic changes and neuroadaptations that may contribute to augmentation. *Sleep Med.* 31 (1), 71–77. <https://doi.org/10.1016/j.sleep.2016.06.003>.
- Egger, M., Smith, G.D., Schneider, M., Minder, C., 1997. Bias in meta-analysis detected by a simple, graphical test. *BMJ* 315 (7109), 629–634. <https://doi.org/10.1136/bmj.315.7109.629>.
- Fazekas, F., Kleinert, R., Offenbacher, H., et al., 1991. The morphologic correlate of incidental punctate white matter hyperintensities on MR images. Published online, *Am J Roentgenol*.
- Ferré, S., Quiroz, C., Guitart, X., et al., 2017. Pivotal role of adenosine neurotransmission in restless legs syndrome. *Front. Neurosci.* 11, 722. <https://doi.org/10.3389/fnins.2017.00722>.
- Fischl, B., 2012. FreeSurfer. *Neuroimage* 62 (2), 774–781. <https://doi.org/10.1016/j.neuroimage.2012.01.021>.
- Godau, J., Schweitzer, K.J., Liepelt, I., Gerloff, C., Berg, D., 2007. Substantia nigra hypoechoic: definition and findings in restless legs syndrome. *Mov. Disord.* 22 (2), 187–192. <https://doi.org/10.1002/mds.21230>.
- Godau, J., Klose, U., Di Santo, A., Schweitzer, K., Berg, D., 2008. Multiregional brain iron deficiency in restless legs syndrome. *Mov. Disord.* 23 (8), 1184–1187. <https://doi.org/10.1002/mds.22070>.
- Gonzalez-Latapi, P., Malkani, R., 2019. Update on restless legs syndrome: from mechanisms to treatment. *Curr. Neurol. Neurosci. Rep.* 19 (8), 54. <https://doi.org/10.1007/s11910-019-0965-4>.
- Greve, D.N., Fischl, B., 2009. Accurate and robust brain image alignment using boundary-based registration. *Neuroimage* 48 (1), 63–72. <https://doi.org/10.1016/j.neuroimage.2009.06.060>.
- Hametner, S., Endmayr, V., Deistung, A., et al., 2018. The influence of brain iron and myelin on magnetic susceptibility and effective transverse relaxation – A biochemical and histological validation study. *Neuroimage* 179, 117–133. <https://doi.org/10.1016/j.neuroimage.2018.06.007>.
- Haschka, D., Volani, C., Stefani, A., et al., 2019. Association of mitochondrial iron deficiency and dysfunction with idiopathic restless legs syndrome. *Mov. Disord.* 34 (1), 114–123. <https://doi.org/10.1002/mds.27482>.
- Higgins, J.P.T., Thompson, S.G., Deeks, J.J., Altman, D.G., 2003. Measuring inconsistency in meta-analyses. *BMJ* 327 (7414), 557–560. <https://doi.org/10.1136/bmj.327.7414.557>.
- Knake, S., Heverhagen, J.T., Menzler, K., Keil, B., Oertel, W.H., Stiasny-Kolster, K., 2010. Normal regional brain iron concentration in restless legs syndrome measured by MRI. *Nat. Sci. Sleep.* 2, 19–22. <https://doi.org/10.2147/NSS.S7040>.
- Koo, B.B., 2015. Restless leg syndrome across the globe. *Sleep Med Clin.* 10 (3), 189–205. <https://doi.org/10.1016/j.jsmc.2015.05.004>.
- Langkammer, C., Krebs, N., Goessler, W., et al., 2010. Quantitative MR imaging of brain iron: a postmortem validation study. *Radiology* 257 (2), 455–462. <https://doi.org/10.1148/radiol.10100495>.
- Langkammer, C., Schweser, F., Krebs, N., et al., 2012. Quantitative susceptibility mapping (QSM) as a means to measure brain iron? A post mortem validation study. *Neuroimage* 62 (3), 1593–1599. <https://doi.org/10.1016/j.neuroimage.2012.05.049>.
- Lanza, G., DelRosso, L.M., Ferri, R., 2022. Sleep and homeostatic control of plasticity. *Handb. Clin. Neurol.* 184, 53–72. <https://doi.org/10.1016/b978-0-12-819410-2.00004-7>.
- Lanza, G., Ferri, R., 2019. The neurophysiology of hyperarousal in restless legs syndrome: Hints for a role of glutamate/GABA. *Adv. Pharmacol.* 84, 101–119. <https://doi.org/10.1016/bs.apha.2018.12.002>.
- Li, X., Allen, R.P., Earley, C.J., et al., 2016. Brain iron deficiency in idiopathic restless legs syndrome measured by quantitative magnetic susceptibility at 7 tesla. *Sleep Med.* 22, 75–82. <https://doi.org/10.1016/j.sleep.2016.05.001>.
- Manconi, M., Govoni, V., De Vito, A., et al., 2004. Restless legs syndrome and pregnancy. *Neurology* 63 (6), 1065–1069. <https://doi.org/10.1212/01.WNL.0000138427.83574.A6>.
- Margariti, P.N., Astrakas, L.G., Tsouli, S.G., Hadjigeorgiou, G.M., Konitsiotis, S., Argyropoulou, M.I., 2012. Investigation of unmedicated early onset restless legs syndrome by voxel-based morphometry, T2 relaxometry, and functional mr imaging during the night-time hours. *Am. J. Neuroradiol.* 33 (4), 667–672. <https://doi.org/10.3174/ajnr.A2829>.
- Mizuno, S., Mihara, T., Miyaoka, T., Inagaki, T., Horiguchi, J., 2005. CSF iron, ferritin and transferrin levels in restless legs syndrome. *J. Sleep Res.* 14 (1), 43–47. <https://doi.org/10.1111/j.1365-2869.2004.00403.x>.
- Mogavero, M.P., Mezzapapa, D.M., Savarese, M., DelRosso, L.M., Lanza, G., Ferri, R., 2021. Morphological analysis of the brain subcortical gray structures in restless legs syndrome. *Sleep Med.* 88, 74–80. <https://doi.org/10.1016/j.sleep.2021.10.025>.
- Möller, H.E., Bossoni, L., Connor, J.R., et al., 2019. Iron, myelin, and the brain: neuroimaging meets neurobiology. *Trends Neurosci.* 42 (6), 384–401. <https://doi.org/10.1016/j.tins.2019.03.009>.
- Moon, H.J., Chang, Y., Lee, Y.S., et al., 2014. T2 relaxometry using 3.0-tesla magnetic resonance imaging of the brain in early- and late-onset restless legs syndrome. *J. Clin. Neurol.* 10 (3), 197–202. <https://doi.org/10.3988/jcn.2014.10.3.197>.
- Moon, H.-J.-J., Chang, Y., Lee, Y.S., et al., 2015. A comparison of MRI tissue relaxometry and ROI methods used to determine regional brain iron concentrations in restless legs syndrome. *Med. Devices (Auckl)* 8, 341–350. <https://doi.org/10.2147/MDER.S83629>.
- Nordlander, N.B., 1953. Therapy in restless legs. *Acta Med. Scand.* 145 (6), 455–457. <https://doi.org/10.1111/j.0954-6820.1953.tb07042.x>.
- R Core Team. R: A Language and Environment for Statistical Computing. *R Found Stat Comput Vienna, Austria*. Published online 2018. <http://www.r-project.org/>.
- Rizzo, G., Manners, D., Testa, C., et al., 2013. Low brain iron content in idiopathic restless legs syndrome patients detected by phase imaging. *Mov. Disord.* 28 (13), 1886–1890. <https://doi.org/10.1002/mds.25576>.
- Rizzo, G., Plazzi, G., 2018. Neuroimaging Applications in Restless Legs Syndrome Vol 143. <https://doi.org/10.1016/bs.im.2018.09.012>.
- Rizzo, G., Li, X., Galantucci, S., Filippi, M., Cho, Y.W., 2017. Brain imaging and networks in restless legs syndrome. *Sleep Med.* 31, 39–48. <https://doi.org/10.1016/j.sleep.2016.07.018>.
- Schmidauer, C., Sojer, M., Seppi, K., et al., 2005. Transcranial ultrasound shows nigral hypoechoic intensity in restless legs syndrome. *Ann Neurol.* 58 (4), 630–634. <https://doi.org/10.1002/ana.20572>.
- Schormair, B., Zhao, C., Bell, S., et al., 2017. Identification of novel risk loci for restless legs syndrome in genome-wide association studies in individuals of European ancestry: a meta-analysis. *Lancet Neurol.* 16 (11), 898–907. [https://doi.org/10.1016/S1474-4422\(17\)30327-7](https://doi.org/10.1016/S1474-4422(17)30327-7).
- Schwarzer, G., Mair, P., Hatzinger, R., 2007. meta: An R package for meta-analysis meta: an R package for meta-analysis. *R News* 7 (3), 40–45.
- Shapiro, S.S., Wilk, M.B., 1965. An analysis of variance test for normality (complete samples). *Biometrika.* 52 (3/4), 591. <https://doi.org/10.2307/2333709>.
- Sidik, K., Jonkman, J.N., 2007. A comparison of heterogeneity variance estimators in combining results of studies. *Stat Med.* 26 (9), 1964–1981. <https://doi.org/10.1002/sim.2688>.
- Snyder, A.M., Wang, X., Patton, S.M., et al., 2009. Mitochondrial ferritin in the substantia nigra in restless legs syndrome. *J. Neuropathol. Exp. Neurol.* 68 (11), 1193–1199. <https://doi.org/10.1097/NEN.0b013e3181bdc44f>.
- Song, F., Hooper, L.Y., 2013. Publication bias: what is it? How do we measure it? How do we avoid it? *Open Access J Clin Trials.* 5 (1), 71. <https://doi.org/10.2147/OAJCT.S34419>.
- Stefani, A., Mitterling, T., Heidbreder, A., et al., 2019. Multimodal Magnetic Resonance Imaging reveals alterations of sensorimotor circuits in restless legs syndrome. *Sleep* 53 (9), 1–30. <https://doi.org/10.1093/sleep/zsz171>.
- Sterne JAC, Sutton AJ, Ioannidis JPA, et al. Recommendations for examining and interpreting funnel plot asymmetry in meta-analyses of randomised controlled trials. *BMJ.* 2011;343(jul22 1):d4002-d4002. [10.1136/bmj.d4002](https://doi.org/10.1136/bmj.d4002).
- Straub, S., Schneider, T.M., Emmerich, J., et al., 2017. Suitable reference tissues for quantitative susceptibility mapping of the brain. *Magn. Reson. Med.* 78 (1), 204–214. <https://doi.org/10.1002/mrm.26369>.
- Treit, S., Naji, N., Seres, P., et al., 2021. R2* and quantitative susceptibility mapping in deep gray matter of 498 healthy controls from 5 to 90 years. *Hum Brain Mapp.* 42 (14), 4597–4610. <https://doi.org/10.1002/hbm.25569>.

- Trenkwalder, C., Allen, R., Högl, B., Paulus, W., Winkelmann, J., 2016. Restless legs syndrome associated with major diseases. *Neurology* 86 (14), 1336–1343. <https://doi.org/10.1212/WNL.0000000000002542>.
- Viechtbauer, W., 2007. Accounting for heterogeneity via random-effects models and moderator analyses in meta-analysis. *Z. Psychol. J. Psychol.* 215 (2), 104–121. <https://doi.org/10.1027/0044-3409.215.2.104>.
- Yang, X., Yang, B., Ming, M., et al., 2019. Efficacy and tolerability of intravenous iron for patients with restless legs syndrome: evidence from randomized trials and observational studies. *Sleep Med.* 61, 110–117. <https://doi.org/10.1016/j.sleep.2019.01.040>.